ELSEVIER

Journal of Alloys and Compounds 356–357 (2003) 109–113

Journal of ALLOYS AND COMPOUNDS

www.elsevier.com/locate/jallcom

Unusual effects on hydrogenation: anomalous expansion and volume contraction

V.A. Yartys[a,*], O. Isnard[b,c], A.B. Riabov[d], L.G. Akselrud[e]

[a]*Institute for Energy Technology, PO Box 40, Kjeller, N-2027, Norway*
[b]*Laboratoire de Cristallographie, associé à l'Université J. Fourier, CNRS, BP 166, 38042 Grenoble Cedex 9, France*
[c]*Institut Universitaire de France, Maison des Universités, 103 boulevard Saint Michel, 75005 Paris, France*
[d]*Physico-Mechanical Institute of the National Academy of Sciences of Ukraine, 5, Naukova Str., Lviv 79601, Ukraine*
[e]*Institute of Inorganic Chemistry, Lviv State University, 6, Kyryla and Mephodiya Str., Lviv 29005, Ukraine*

Received 15 July 2002; accepted 21 November 2002

Abstract

The present paper considers two unique volume effects associated with the formation of intermetallic hydrides, anomalously high linear and volume expansion ($CeNi_3 \rightarrow CeNi_3D_{2.8}$) and unusual volume contraction ($HoNiSn \rightarrow HoNiSnD_{0.67}$). The crystal structures of both deuterides were solved on the basis of powder neutron diffraction data. The hexagonal $CeNi_3$ anisotropically expands on hydrogenation along 00*z* (30.7%). In orthorhombic $CeNi_3D_{2.8}$ (space group *Pmcn* (No. 62); $a=4.8748(3)$; $b=8.5590(5)$; $c=21.590(2)$ Å) this expansion proceeds within the $CeNi_2$ slabs only (63.1%), with a 'shrinking' of the $CeNi_5$ parts (−2.8%). All D atoms are located inside the $CeNi_2$ part and on the border of $CeNi_2$ and $CeNi_5$. In sharp contrast to the known crystal structures of intermetallic hydrides, in $CeNi_3D_{2.8}$ deuterium atoms do not fill initially existing interstices but, instead, attract cerium atoms into their surrounding and form new D-occupied sites, Ce_3Ni and Ce_3Ni_3. The hydrogenation of HoNiSn causes a transition from TiNiSi to the ZrNiAl type of structure. Transformation of the metallic sublattice into the ZrNiAl type results in a 'shrinking' of the Ho_3Ni tetrahedra filled by D. Their occupation in $HoNiSnD_{0.67}$ (space group $P\bar{6}2m$ (No. 189); $a=7.24197(10)$; $c=3.93514(7)$ Å) proceeds with a formal 'negative' volume expansion effect and leads to the formation of strong Ho–H bonds.

Keywords: Hydrogen storage materials; Gas–solid reactions; Neutron diffraction; X-ray diffraction; Crystal structure and symmetry

1. Introduction

Formation of intermetallic hydrides is typically accompanied by a volume expansion equivalent to 2.5–3.0 $Å^3$ per absorbed hydrogen atom. The most frequent situation is associated with a unilateral expansion in the so-called 'isotropic' structures. In contrast, a pronounced linear expansion along a sole crystallographic direction takes place in 'anisotropic' structures. In the recently studied new type of intermetallic hydrides, $RE_3Ni_3In_3D_4$ [1], a pair of hydrogen atoms with unusually short H–H separation of ~1.6 Å was found. From a structural point of view, in $RE_3Ni_3In_3D_4$ the appearance of short H–H distances correlates with an anisotropic uniaxial lattice expansion on hydrogenation (16%). Thus, it is important to study the hydrides where this feature is even more pronounced.

The most interesting example of 'anisotropic' structures represents hexagonal (trigonal) hydrides formed on the basis of RT_3 intermetallics in the binary systems of rare earth metals with nickel and cobalt. During hydrogenation, an anomalously large expansion occurs in the [001] direction. It reaches 32% and has been observed for $(La,Ce,Pr,Nd)Ni_3H_{3-4}$ and $CeCo_3H_4$ [2–4]. In $HoNi_3D_{1.8}$ [5], RCo_3D_4 (R=Y, Er) [6] and $(Y,Ce)Ni_3D_x$ [7,8] so far studied by powder neutron diffraction, the anisotropic expansion effect is relatively small in comparison with $(La,Ce,Pr,Nd)Ni_3H_{3-4}$ and $CeCo_3H_4$.

The other extreme case associated with volume changes on hydrogenation is observed in the series of RNiSn intermetallics and their corresponding hydrides. Here the expansion effects gradually decrease from 7.9 vol.% observed for $LaNiSnD_2$ [9] to 2–3% for the compounds of heavier rare earths (f.e., 1.9% for NdNiSnD [10]) and

*Corresponding author. Tel.: +47-6380-6453; fax: +47-6381-2905.
E-mail address: volodymyr.yartys@ife.no (V.A. Yartys).

0925-8388/03/$ – see front matter
doi:10.1016/S0925-8388(03)00106-3

become negative values for (Ho,Er)NiSn [11]. The reasons for such unusual behavior need to be established.

This work was based on studies by means of high resolution powder neutron diffraction of two unusual effects on hydrogenation: anomalous expansion and volume contraction considering cases of $CeNi_3D_{2.8}$ and $HoNiSnD_{0.67}$. The structural studies revealed the existence of new, previously undescribed phenomena in the metal–hydrogen systems.

2. Experimental

$CeNi_3$ and HoNiSn intermetallic alloys were prepared from the high purity constituent elements by arc melting under argon gas atmosphere. $CeNi_3$ was subsequently annealed at 900 °C for 3 weeks and water-quenched after the annealing. HoNiSn was used in as-cast condition. Deuteration was performed at room temperature and D_2 pressures not exceeding 10 bar ($CeNi_3$), or at 3–4 bar D_2 pressures and temperatures of 400–450 °C (HoNiSn). Powder neutron diffraction (PND) data of $CeNi_3D_{2.8}$ (the sample was sealed in the quartz autoclave) were collected at the high resolution diffractometer D1A, Institut Laue Langevin (ILL), using the wavelength 1.911 Å. The PND data for $HoNiSnD_{0.67}$ (sample was sealed under argon in the 5-mm vanadium sample holder) were measured on the D1B instrument ($\lambda = 2.52$ Å), ILL. The step increments of the diffraction angle 2θ were 0.05° (D1A) and 0.2° (D1B). The refinements of the data were performed with the GSAS software [12] using the neutron scattering lengths taken from the GSAS library. XRD characterisation of the alloys and their hydrides was performed using a Siemens D 5000 diffractometer (Cu $K\alpha_1$ radiation). Synchrotron XRD data were collected at high resolution diffractometer at the Swiss-Norwegian Beam Line, ESRF (monochromatic X-rays with $\lambda = 0.50056$ Å).

3. Results and discussion

3.1. Crystal chemical analysis of the intermetallic compound $CeNi_3$ and HoNiSn

The crystal structure of $CeNi_3$ (own structure type) can be considered as a stacking of the $CaCu_5$- and $MgZn_2$-type slabs along [001]. Combination $1*RT_5 + 2*RT_2$ provides the overall stoichiometry $3*RNi_3$. $CeNi_3$ structure contains 12 types of tetrahedral sites with three kinds of surrounding, Ce_2Ni_2, $CeNi_3$ and Ni_4. A non-uniform expansion of $CeNi_5$ and $CeNi_2$ slabs is the most probable scenario following an anisotropic expansion of the unit cell in the [001] direction.

Orthorhombic HoNiSn crystallises with TiNiSi-type structure. The unit cell of intermetallic alloy contains two types of interstices, Ho_3Ni tetrahedra and Ho_3 triangles (both four per unit cell), which can be filled by H atoms (maximum composition of 2 at.H/f.u.HoNiSn will be reached). These sites are too large (Ho_3Ni tetrahedron: $r = 0.59$ Å; Ho_3 triangle: $r = 0.72$ Å) to accommodate H atoms, so a significant deformation of the metal sublattice can be expected with hydrogenation.

3.2. Crystal structure of $CeNi_3D_{2.8}$

The crystal structure of the initial hexagonal intermetallic alloy $CeNi_3$ (space group $P6_3/mmc$; $a = 4.96461(8)$; $c = 16.5213(3)$ Å) refined from the PND showed good agreement with the reference data [13].

X-ray diffraction study of $CeNi_3D_{2.8}$ shows a pronounced linear expansion of the hexagonal unit cell along **c**, $\Delta c/c = 30.7\%$. At the same time, lattice contracts in the basal plane by 0.5–1.8% and undergoes an orthorhombic deformation ($a = 4.8748(3)$; $b = 8.5590(5)$; $c = 21.590(2)$ Å; $a_{orth} = a_{hex}$; $b_{orth} = a_{hex} * \sqrt{3}$; $b_{orth}/a_{orth} = 1.756$; $\Delta a/a \neq \Delta b/a_{hex} * \sqrt{3}$). From group–subgroup relations and observed extinctions, the space group of symmetry was deduced as $Pmcn$ ($P6_3/mmc \rightarrow Cmcm \rightarrow Pmcn$ ($Pnma$)). Rietveld plot of powder neutron diffraction data for $CeNi_3D_{2.8}$ is shown in Fig. 1. Crystal structure data for $CeNi_3D_{2.8}$ are presented in Table 1.

In orthorhombic $CeNi_3D_{2.8}$ the lattice elongation proceeds within the $CeNi_2$ slabs only (63.1%), with a 'shrinking' of the $CeNi_5$ parts (−2.8%). Such extremely large expansion as for the $CeNi_2$ part is uniquely high. Similar effects have not been reported in publications on metal hydrides so far. As a result, a complete rebuilding of the metal sublattice takes place. This rebuilding is easily seen if one compares the modifications of the chains of Ni_4 and $CeNi_3$ tetrahedra aligned along [001]. In the $CeNi_3$ intermetallic compound the Ni_4 tetrahedra are nearly regular. In contrast, after the expansion to form $CeNi_3D_{2.8}$ some of these tetrahedra become so expanded that they do

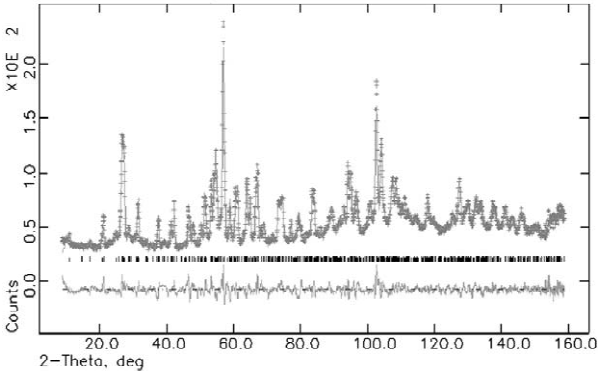

Fig. 1. Powder neutron diffraction pattern for $CeNi_3D_{2.8}$ (D1A instrument, $\lambda = 1.911$ Å) showing observed (dots), calculated (line) and difference (line at bottom) pattern. Positions of the peaks are marked. $R_p = 4.78\%$; $R_{wpr} = 6.35\%$; $\chi^2 = 4.94$. Diffuse background originates from the quartz sample container.

Table 1
Crystal structure data for $CeNi_3D_{2.8}$

Atom	Site	x	y	z	D surrounding
Ce1	4c	1/4	0.430(3)	0.2514(9)	
Ce2	4c	1/4	0.378(2)	0.0575(6)	
Ce3	4c	1/4	0.087(4)	0.9364(8)	
Ni1	4c	1/4	0.755(1)	0.5297(4)	
Ni2	4c	1/4	0.929(2)	0.3348(6)	
Ni3	4c	1/4	0.748(1)	0.2461(6)	
Ni4	4c	1/4	0.086(1)	0.2555(5)	
Ni5	4c	1/4	0.938(1)	0.1564(5)	
Ni6	8d	0.005(2)	0.8219(10)	0.8392(3)	
Ni7	8d	0.497(2)	0.1774(11)	0.3532(3)	
D1	4c	1/4	0.726(2)	0.8894(8)	$Ce2_2Ce3Ni2Ni6_2$
D2	4c	1/4	0.080(1)	0.1120(5)	$Ce2Ce3_2Ni5Ni6_2$
D3	4c	1/4	0.916(1)	0.4962(7)	$Ce2_3Ni1$
D4	4c	1/4	0.233(1)	0.6498(5)	$Ce1Ce2Ni6_2$
D5	8d	−0.030(2)	0.169(1)	0.0094(4)	$Ce2Ce3_2Ni1$
D6	4c	1/4	0.771(3)	0.1007(5)	$Ce3_2Ni1Ni5Ni7_2$
D7	4c	1/4	0.971(2)	0.4180(10)	$Ce2_2Ce3Ni2Ni7_2$
D8[a]	4c	1/4	0.478(1)	0.1514(8)	$Ce1Ce2Ni7_2$

Space group *Pmcn* (No. 62). Unit cell parameters: $a=4.8748(3)$; $b=8.5590(5)$; $c=21.590(2)$ Å. $T=300$ K. Data recorded on the D1A diffractometer.
[a] Occupancy 0.30 (3).

not exist any more (Fig. 2a and b). The same conclusion is reached for the $CeNi_3$ sites aligned along [001]: Ce–Ni bonding is broken in the 00*z* direction.

Occupancy/vacancy of the $CeNi_2$ and $CeNi_5$ parts by deuterium is in agreement with the observed values of volume expansion. All D atoms are located inside the $CeNi_2$ part and on the border of $CeNi_2$ and $CeNi_5$ leaving $CaCu_5$-type part empty. Deuterium atoms occupy eight different sites, with seven of eight (D1–D7) being completely filled. Observed stoichiometry is $CeNi_3D_{2.765}$. If all eight sites are completely occupied, this will cause stoichiometry to increase to $D/CeNi_3=3.0$.

In sharp contrast to the known crystal structures of intermetallic hydrides, in $CeNi_3D_{2.8}$ deuterium atoms do not fill *initially existing* interstices but, instead, attract cerium atoms into their surrounding and form *new D-occupied sites*, Ce_3Ni and Ce_3Ni_3 (Fig. 3a and b). In addition, the 'regular' Ce_2Ni_2 and Ce_2Ni_4 sites are filled. From eight D sites two have surrounding Ce_3Ni, three Ce_2Ni_2, two Ce_3Ni_3 and one Ce_2Ni_4. In $CeNi_3D_{2.8}$ D sublattice is completely ordered with all D–D distances exceeding 1.80 Å. This sublattice can be presented as a stacking of the coordination polyhedra of two types, polyhedra with 12 vertices and polyhedra with seven vertices formed by D around Ce2 and Ce3 atoms from the $CeNi_2$ slab (Fig. 4).

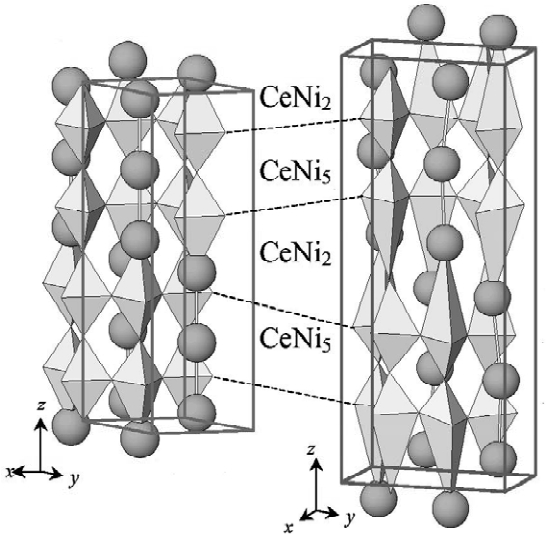

Fig. 2. Framework of Ni_4 and $CeNi_3$ tetrahedra aligned along [001] in the structures of $CeNi_3$ (a) and $CeNi_3D_{2.8}$ (b). $CeNi_2$ ($MgZn_2$-type) and $CeNi_5$ ($CaCu_5$-type) slabs are shown. For comparison, $CeNi_3$: hexagonal: $a=4.96461(8)$; $c=16.5213(3)$ Å; $d_{Ni-Ni}=2.54$ Å; $d_{Ce-Ni}=3.14$ Å; $CeNi_3D_{2.8}$: orthorhombic: $a=4.8748(3)$; $b=8.5590(5)$; $c=21.590(2)$ Å; $d_{Ni-Ni}=4.34$–4.45 Å; $d_{Ce-Ni}=4.60$–5.08 Å.

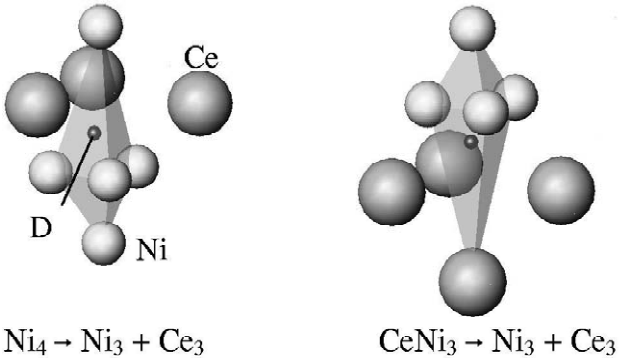

Fig. 3. Deuterium atoms formally located inside the Ni_4 (a) and $CeNi_3$ (b) tetrahedra bring three cerium atoms into their surrounding changing D coordination to Ce_3Ni_3. Ni_4 and $CeNi_3$ tetrahedra do not exist any more, because of extremely large elongation of the Ni–Ni (2.54→4.34–4.45 Å) and Ce–Ni (3.14→4.60–5.08 Å) interatomic distances.

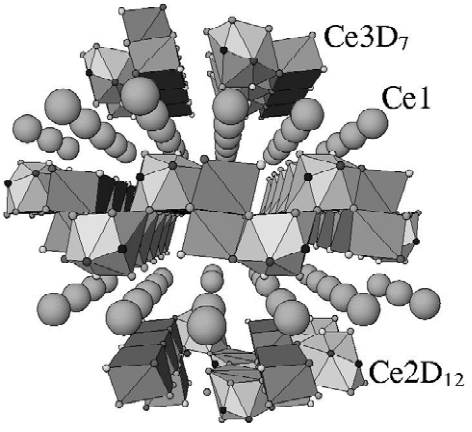

Fig. 4. Hydrogen sublattice in the structure of $CeNi_3D_{2.8}$ shown along [001] as a stacking of the polyhedra ($Ce2D_{12}$ and $Ce3D_7$) formed by D atoms around the Ce atoms inside the $CeNi_2$ slabs. Ce1 atoms inside the $CeNi_5$ slabs are weakly bound to hydrogen.

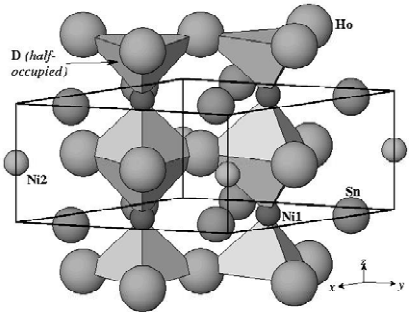

Fig. 5. Crystal structure of $HoNiSnD_{0.67}$.

The hydrogenation behavior of the constituent parts of $CeNi_3$, $CeNi_5$ and $CeNi_2$, reveals differences in comparison with corresponding binary intermetallic compounds. $CeNi_2$ cubic Laves phase becomes amorphous on hydrogenation [14] while $CeNi_5$-based hydride at room temperature decomposes at pressures below 48 bar [15]. In contrast, $CeNi_5$ parts stabilise the $CeNi_2$ parts in $CeNi_3$, and a good crystalline $CeNi_3D_{2.8}$ hydride is formed. In turn, $CeNi_5$ parts in $CeNi_3$ become involved in the hydrogenation process at the rather low pressure of 1 bar D_2, as a result of the influence of the $CeNi_2$ parts connected to them.

Volume effects, which are observed on the transformation $CeNi_3 \rightarrow CeNi_3D_{2.8}$, do not seem to be associated with the changes of the valence state of cerium on hydrogenation. This conclusion is based on the similarities between $CeNi_3D_{2.8}$ ($\Delta c/c = 30.7\%$; $\Delta V/V = 27.7\%$) and $LaNi_3H_4$ ($\Delta c/c = 32.0\%$; $\Delta V/V = 29.7\%$) [16]. In the latter case, no valence changes during the hydride formation take place, however the observed effects resemble the behavior of the $CeNi_3$–H_2 system.

3.3. Crystal structure of $HoNiSnD_{0.67}$

A completely opposite situation with respect to volume changes is observed in the system HoNiSn–D_2. Here SR XRD study of $HoNiSnD_{0.67}$ showed that deuterium absorption is accompanied by a volume *contraction* of 0.64% (HoNiSn at 293 K: space group *Pnma*; $a = 7.0682(9)$; $b = 4.4396(6)$; $c = 7.6433(9)$ Å; $V = 239.85$ Å^3; $HoNiSnD_{0.67}$ at 293 K: space group $P\bar{6}2m$; $a = 7.2420(2)$; $c = 3.93514(7)$ Å; 4/3 $V = 238.31$ Å^3). This contraction is associated with structural phase transition from TiNiSi to the hexagonal ZrNiAl-type structure. The instability of the TiNiSi structure with respect to insertion of interstitial atoms causes its transformation to the ZrNiAl-type structure. The latter RNiX structure contains trigonal bipyramids R_3Ni_2 which are occupied by D in the structure of $TbNiAlD_{0.54}$ [17]. PND study of $HoNiSnD_{0.67}$ showed that at similar deuterium concentration in the intermetallic lattice deuterium atoms are shifted from the centers of these sites into the side-connected Ho_3Ni1 tetrahedra which share a common triangular Ho_3 face (Fig. 5, Table 2). The radii of these occupied Ho_3Ni1 sites are much smaller (0.46 Å) compared to the original structure. As shown by thermal desorption spectroscopy studies, this, in turn, allows the formation of strong Ho–D bonds. These bonds are broken in vacuum at temperatures above 500 °C, which are unusually high for the intermetallic hydrides.

Because of short separation between the centers of the Ho_3Ni1 tetrahedra they are half-occupied at maximum. A shift of D atom from the center of bipyramid into the tetrahedron increases Ho–D distance to 2.23 Å, while Ni1–D distance (1.66 Å) falls into the range typical for such distances in the structures of Ni-containing intermetallic hydrides.

Volume contraction is known to take place in the binary M–H systems with a substantial degree of ionic bonding between metals and hydrogen. However, in the case of HoNiSn and $HoNiSnD_{0.67}$, both compounds exhibit similar magnetic properties [18] indicating absence of significant modifications of the electronic structure on H absorption.

Table 2
Crystal structure data for $HoNiSnD_{0.67}$

Atom	Site	*x*	*y*	*z*	D surrounding
Ho	3*g*	0.5984(3)	0	$\frac{1}{2}$	
Ni1	2*c*	1/3	2/3	0	
Ni2	1*b*	0	0	$\frac{1}{2}$	
Sn	3*f*	0.259(2)	0	0	
D[a]	4*h*	1/3	2/3	0.58(2)	Ho_3Ni1

Space group $P\bar{6}2m$ (No. 189). $a = 7.240(2)$; $c = 3.936(1)$ Å. $T = 230$ K. Data recorded on the D1B diffractometer.

[a] Occupancy 0.50 (–).

4. Conclusions

New interesting structural behaviours have been observed during powder neutron diffraction studies of intermetallic hydrides formed in the systems $CeNi_3$–D_2 and HoNiSn–D_2. Despite the volume effects on hydrogenation being opposite in sign, they have a common feature. This feature is a significant rebuilding of the metal sublattice resulting from dominating the hydrogenation behaviours of the materials interactions of atoms of the rare earth metals and hydrogen. The structural modifications observed on the hydrogenation of $CeNi_3$ and HoNiSn are not caused by the changes in the valence state of the constituent rare earth metals. In both studied hydrides, instead of filling the existing interstitial sites, hydrogen induces structural transformations leading to the structural phase transition in HoNiSn–D_2 and to the creation of significantly different surrounding for hydrogen atoms in $CeNi_3D_{2.8}$ in comparison with the initial intermetallic $CeNi_3$. In the latter case hydrogen–cerium interactions bring cerium into the neighborhood of D instead of Ni. Because of anisotropic expansion, certain interstices become so expanded that they do not exist any more. That is why on hydrogenation the behavior of the constituent parts of $CeNi_3$, $CeNi_5$ and $CeNi_2$, becomes different from the corresponding binary intermetallic compounds.

Further studies on structurally unusual intermetallic hydrides are necessary to understand better the H storage behaviours of intermetallic hydrides.

Acknowledgements

This work has received support from the Research Council of Norway and from Norsk Hydro ASA. We sincerely thank R.V. Denys for his help in the preparation of the alloys. We are indebted to the Institut Laue Langevin of Grenoble, France for the provision of neutron facilities. The skillful assistance from the project team at the Swiss-Norwegian Beam Line, ESRF is gratefully acknowledged.

References

[1] V.A. Yartys, R.V. Denys, B.C. Hauback, H. Fjellvåg, I.I. Bulyk, A.B. Riabov, Yu.M. Kalychak, J. Alloys Comp. 330–332 (2002) 132.
[2] R.H. van Essen, K.H.J. Buschow, J. Less-Common Met. 70 (1980) 189.
[3] V.V. Burnasheva, B.P. Tarasov, Zh. Neorg. Khim. 27 (1982) 1908.
[4] V.A. Yartys, V.V. Burnasheva, K.N. Semenenko, Adv. Chem. 52 (1983) 529.
[5] S.P. Solovyov, N.V. Fadeeva, V.A. Yartys, V.V. Burnasheva, K.N. Semenenko, Phys. Tverd. Tela 23 (1981) 1226.
[6] M.I. Bartashevich, A.N. Pirogov, V.I. Voronin, T. Goto, M. Yamaguchi, I. Yamamoto, J. Alloys Comp. 231 (1–2) (1995) 104.
[7] M. Latroche, A. Percheron-Guégan, in: Abstract book of International Symposium on Metal–Hydrogen Systems. Fundamentals and Applications. Annecy, France, 2–6 September 2002, p. 30.
[8] M. Latroche, Y. Chabre, A. Percheron-Guégan, O. Isnard (unpublished).
[9] V.A. Yartys, T. Olavesen, B.C. Hauback, H. Fjellvåg, H.W. Brinks, J. Alloys Comp. 330–332 (2002) 141.
[10] V.A. Yartys, T. Olavesen, B.C. Hauback, H. Fjellvåg, J. Alloys Comp. 336 (1–2) (2002) 181.
[11] V.A. Yartys, in: 8th European Conference on Solid State Chemistry, Oslo, July 2001, Program (Part I), p. I-6.
[12] A.C. Larson, R.B. von Dreele, General Structure Analysis System (GSAS), LANSCE, MS-H 805 (1994).
[13] D.T. Cromer, C.E. Olsen, Acta Crystallogr. 12 (1959) 689.
[14] V. Paul-Boncour, C. Lartigue, A. Percheron-Guégan, J.C. Achard, J. Pannetier, J. Less-Common Met. 143 (1988) 301.
[15] F. Pourarian, W.E. Wallace, Int. J. Hydr. Energy 10 (1985) 49.
[16] V.V. Burnasheva, B.P. Tarasov, K.N. Semenenko, Zh. Neorg. Khim. 27 (12) (1982) 3039.
[17] H.W. Brinks, V.A. Yartys, B.C. Hauback, H. Fjellvåg, J. Alloys Comp. 330–332 (2002) 169.
[18] A. Szytula, O. Isnard, V.A. Yartys (unpublished).